

Fingerprint of topological Andreev bound states in phase-dependent heat transport

Björn Sothmann¹ and Ewelina M. Hankiewicz¹

¹*Institute for Theoretical Physics and Astrophysics,
University of Würzburg, Am Hubland, 97074 Würzburg, Germany*

(Dated: January 27, 2023)

We demonstrate that phase-dependent heat currents through superconductor-topological insulator Josephson junctions provide a useful tool to probe the existence of topological Andreev bound states, even for multi-channel surface states. We predict that in the tunneling regime topological Andreev bound states lead to a minimum of the thermal conductance for a phase difference $\phi = \pi$, in clear contrast to a maximum of the thermal conductance at $\phi = \pi$ that occurs for trivial Andreev bound states in superconductor-normal metal junctions. This opens up an unexplored avenue where phase-dependent heat transport can distinguish between topologically trivial and nontrivial 4π modes. Furthermore, we propose a SQUID geometry where phase-dependent heat currents can be measured using available experimental technology.

Introduction.— At the interface between a normal metal and a superconductor, an electron with an energy inside the superconducting gap gets reflected from the superconductor as a hole in a process called Andreev reflection [1]. In a superconductor-normal metal-superconductor (S-N-S) junction, this electron-hole conversion leads to the formation of Andreev bound states with discrete energies [2]. In the case of a short, one-dimensional junction there is exactly one pair of such bound states with energy $\varepsilon = \pm\Delta\sqrt{1 - D\sin^2\phi}/2$ where D denotes the transmission probability of the junction in the normal state, Δ is the absolute value of the superconducting pair potential and ϕ the phase difference across the junction [3].

Recently, there has been a growing interest in Josephson junctions based on topological insulators (TIs). The surface states of a three-dimensional TI give rise to the formation of topologically nontrivial helical Andreev bound states with energy $\varepsilon = \pm\Delta\cos\phi/2$ [4], i.e., they exhibit a zero-energy crossing at $\phi = \pi$. In contrast to the S-N-S case where even weak backscattering leads to a splitting of the accidental degeneracy of Andreev bound states at $\phi = \pi$, the crossing in the S-TI-S case is robust due to topological protection. It gives rise to a 4π -periodic Josephson current [5]. The latter is difficult to observe in experiment [6, 7] as it is a single-channel effect and subject to quasiparticle poisoning. Although recent experiments provide some evidence for the existence of helical Andreev bound states in the non-sinusoidal current phase relation [8], in the diffraction pattern [9] and missing Shapiro steps in the AC Josephson effect [10], it is still an outstanding challenge to distinguish between topologically trivial and nontrivial 4π modes.

Interestingly, not only the Josephson current but also the heat current between two superconductors kept at different temperatures depends on the phase difference across the junction. The effect arises due to the interference between quasiparticles carrying heat and Cooper pairs carrying phase information. It was theoretically

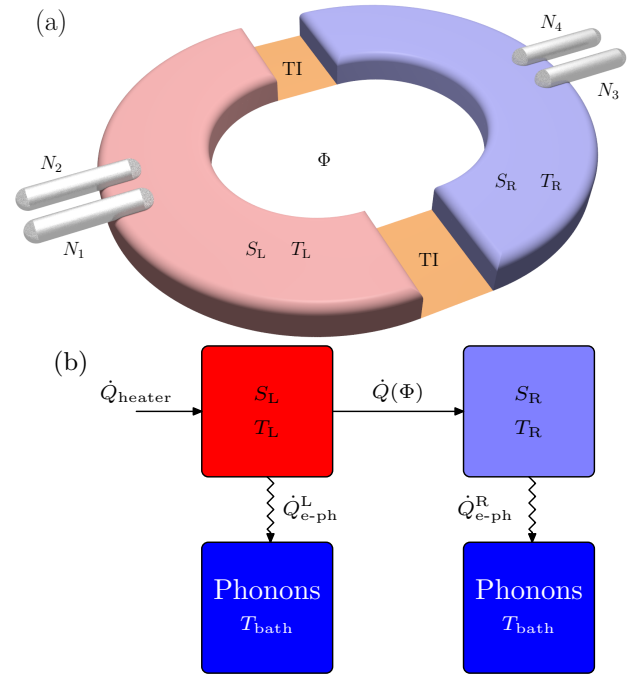


FIG. 1. (a) SQUID geometry to detect phase-dependent heat currents. A magnetic flux Φ controls the phase difference across two identical Josephson junctions connecting superconductors S_L and S_R at temperatures T_L and T_R , respectively. Normal metal contacts N_{1-4} serve as heater and thermometer for the left and right superconductor, respectively. (b) Thermal model accounting for heat flows, see text for details.

predicted for tunnel junctions [11–15] as well as for point contacts with arbitrary transmission [16, 17]. Phase-dependent heat currents can be used as an alternative approach to probe Andreev bound states. Indeed their effects have been very recently observed experimentally in a superconducting quantum interference device (SQUID) based on S-N-S junctions [18]. Subsequent experiments demonstrated the diffraction of heat currents in large junctions subject to magnetic fields [19] and realized a

double SQUID that allows for enhanced control of heat flows [20]. Theoretically, phase-dependent heat transport has been investigated in ferromagnetic Josephson junctions [21, 22] as well as for AC-driven systems [23]. Furthermore, the fluctuations of phase-dependent heat currents [24] and their influence on the dephasing of flux qubits [25] have been studied.

In this Letter, we demonstrate that phase-dependent heat currents provide a robust tool to probe the existence of topological Andreev bound states in S-TI-S Josephson junctions as well as to distinguish them from trivial 4π periodic Andreev bound states. Since heat currents are carried by quasiparticles with energies above or below the superconducting gap, they provide complementary information to the Josephson current which is due to the formation of Andreev bound states within the gap. For the same reason, heat transport does not suffer from quasiparticle poisoning in contrast to the 4π -periodic Josephson effect. We find that the thermal conductance carries clear signatures of the helical Andreev bound states both for short and long junctions as well as in the one-dimensional and two-dimensional case. Finally, we propose an experimental setup based on a SQUID, cf. Fig. 1, that allows for the detection of phase-dependent heat currents within the reach of state-of-the-art experimental technology.

Model.— We consider a ballistic Josephson junction based on the surface states of a three-dimensional TI in the $x-y$ plane. The areas $|x| > L/2$ are covered by conventional BCS superconductors with pair potential $\Delta e^{i\phi_r}$ where ϕ_r is the phase of superconductor $r = \text{L,R}$ such that there is a phase difference $\phi = \phi_{\text{R}} - \phi_{\text{L}}$ across the junction. For $|x| < L/2$, the pair potential vanishes, $\Delta = 0$. We assume that the pair potential changes on a length scale much shorter than the superconducting coherence length. This allows us to approximate the pair potential as a step function at the S-TI interface. We, furthermore, neglect proximity effects that would require a self-consistent determination of the pair potential.

Electron- and hole-like quasiparticles are described by the Bogoliubov-de Gennes Hamiltonian

$$H = \begin{pmatrix} \hat{h}_{\mathbf{k}} & i\hat{\sigma}_y \Delta e^{i\phi_r} \\ -i\hat{\sigma}_y \Delta e^{-i\phi_r} & -\hat{h}_{-\mathbf{k}}^* \end{pmatrix}, \quad (1)$$

acting on wave functions describing electron- and hole-like quasiparticles with spin \uparrow and \downarrow . The single-particle Dirac Hamiltonian $\hat{h}_{\mathbf{k}} = \hbar v_{\text{F}} \mathbf{k} \cdot \hat{\boldsymbol{\sigma}} - \mu \hat{\sigma}_0$ describes the helical surface states of the TI in the absence of superconductivity where v_{F} is the Fermi velocity, \mathbf{k} the charge carrier wave vector, $\hat{\boldsymbol{\sigma}}$ the vector of Pauli matrices in spin space with σ_0 denoting the unit matrix and μ the chemical potential.

The eigenfunctions of the Bogoliubov-de Gennes Hamiltonian describing right-moving electron- and hole-like quasiparticles of energy ω are given by $\psi_1(x, y) =$

$(u, e^{i\theta_e} u, -e^{-i\phi_r} e^{i\theta_e} v, e^{-i\phi_r} v)^T e^{i\mathbf{k}_e \cdot \mathbf{r}}$ and $\psi_2(x, y) = (v, e^{i\theta_h} v, e^{-i\phi_r} e^{i\theta_h} u, e^{-i\phi_r} u)^T e^{i\mathbf{k}_h \cdot \mathbf{r}}$, respectively, where $\mathbf{r} = (x, y)$, $\mathbf{k}_{e,h} = k_{e,h}(\cos \theta_{e,h}, \sin \theta_{e,h})$, and $u = \frac{1}{2} \sqrt{1 + \frac{\sqrt{\omega^2 - \Delta^2}}{\omega}}$ and $v = \frac{1}{2} \sqrt{1 - \frac{\sqrt{\omega^2 - \Delta^2}}{\omega}}$ denote the usual coherence factors. The eigenfunctions $\psi_3(x, y)$ and $\psi_4(x, y)$ describing left-moving quasiparticles are obtained from $\psi_1(x, y)$ and $\psi_2(x, y)$ by replacing the angle of incidence $\theta_{e,h}$ with $\pi - \theta_{e,h}$. In the following, we will assume that the superconducting regions are heavily doped, $\mu \gg \Delta, \omega$, such that we can approximate $k_e = k_h \equiv k_{\text{S}}$ and $\theta_e = \theta_h \equiv \theta_{\text{S}}$.

Let us now consider the situation of an electron-like quasiparticle incident from the left-hand side. It gives rise to reflected and transmitted electron- and hole-like quasiparticles such that the wave function in the two superconductors reads $\psi_{\text{L}}(x, y) = \psi_1(x, y) + r_e \psi_3(x, y) + r_e \psi_4(x, y)$ and $\psi_{\text{R}}(x, y) = t_e \psi_1(x, y) + t_h \psi_2(x, y)$, respectively. For a short junction, $L = 0$, we model the interface barrier by the delta potential, $U\delta(x)$, with barrier height U , although our results are qualitatively independent of the barrier shape. The potential leads to the boundary condition $\psi_{\text{L}}(0, y) = (\cos Z \hat{\tau}_0 \hat{\sigma}_0 + i \sin Z \hat{\tau}_z \hat{\sigma}_x) \psi_{\text{R}}(0, y)$ where $Z = U/\hbar v_{\text{F}}$ and $\hat{\boldsymbol{\tau}}$ denotes the vector of Pauli matrices in particle-hole space. In a long junction, scattering arises due to the wave vector mismatch between the normal and superconducting region. For simplicity, we assume that there is no additional potential barrier at the interface. Thus, in this case, wave functions are continuous at the interface. From the boundary conditions, the transmission amplitudes t_e and t_h and subsequently the transmission probability for an electron-like quasiparticle $\mathcal{T}_e(\omega, \phi) = |t_e|^2 + |t_h|^2$ can be determined.

The thermal conductance of a one-dimensional Josephson junction is given by

$$\kappa(\phi) = \frac{2}{h} \int_{\Delta}^{\infty} d\omega \omega \mathcal{T}_e(\omega, \phi) \frac{df}{dT}, \quad (2)$$

where $f = [\exp(\omega/k_{\text{B}}T) + 1]^{-1}$ denotes the equilibrium Fermi distribution. For a two-dimensional Josephson junction, one has to perform an additional average over $\sin \theta_{\text{S}}$ and multiply with the number $N \gg 1$ of open transport channels.

Short junction.— For a short, one-dimensional S-TI-S junction, the transmission probability of an electron-like quasiparticle is given by

$$\mathcal{T}_e(\omega, \phi) = \frac{\omega^2 - \Delta^2}{\omega^2 - \Delta^2 \cos^2 \frac{\phi}{2}}. \quad (3)$$

It is independent of the potential barrier at the interface, similarly to superconducting Klein tunneling for Andreev bound states [26]. In consequence, the thermal conductance of the junction exhibits a universal behaviour independent of the interface scattering, cf. Fig. 2(a). In the limit $x = \Delta/k_{\text{B}}T \gg 1$, we obtain the analytical approxi-

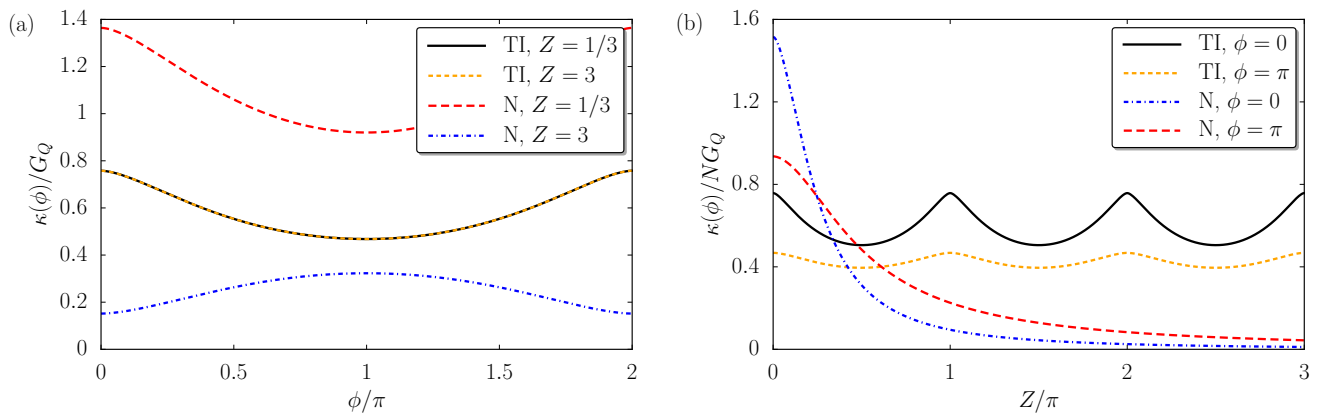


FIG. 2. (a) Phase-dependence of the thermal conductance in units of the thermal conductance quantum $G_Q = \pi^2 k_B^2 T / (3h)$ for short, one-dimensional S-N-S and S-TI-S Josephson junctions for different interface barrier strength Z . (b) Thermal conductance for short, two-dimensional S-N-S and S-TI-S Josephson junctions with $N \gg 1$ channels as a function of the interface barrier strength. The temperature is chosen as $k_B T = \Delta/2$.

mation

$$\kappa(\phi = 0) = \frac{2k_B^2 T}{h} (x^2 + 2x + 2)e^{-x}, \quad (4)$$

$$\kappa(\phi = \pi) = \frac{4k_B^2 T}{h} (x + 1)e^{-x}, \quad (5)$$

i.e., lowering the temperature increases the amplitude of the thermal conductance oscillations but also reduces the total heat flow due to the reduced number of thermally excited quasiparticles.

The phase-dependence of the S-TI-S junction is in clear contrast to the S-N-S case. The latter exhibits a transition from a minimal thermal conductance at $\phi = \pi$ for a transparent interface to a maximal thermal conductance at $\phi = \pi$ in the tunneling limit [16, 17], cf. Fig. 2(a). The different behaviors can be understood by analyzing the density of states at the interface. For a S-TI-S junction, the density of states is given by

$$\rho(\omega) = \rho_N \mathcal{T}_e(\omega, \phi) \frac{|\omega|}{\sqrt{\omega^2 - \Delta^2}}, \quad (6)$$

where ρ_N is the interface density of states in the normal state. At $\phi = 0$, we recover the usual BCS density of states with a singularity at $\omega = \Delta$ due to the topological Andreev bound states merging with the continuum, similar to the S-N-S junction. For transparent S-N-S and S-TI-S junctions the low-energy Andreev bound states remove density of states from above the gap leading to a reduced thermal conductance. However, in the tunneling regime S-TI-S junctions show strikingly different behaviour from S-N-S junctions. This is because helical Andreev bound states are protected by time-reversal symmetry against backscattering independent of the height of the barrier [26, 27]. Therefore, they always stay in the middle of the superconducting gap leading to the suppression of the density of states and the minimum in

thermal conductance for $\phi = \pi$. This is in clear contrast to the S-N-S junction, where the Andreev bound states shift to the edge of the superconducting gap leading to an enhancement of the thermal conductance at $\phi = \pi$ [16, 17].

Due to their simplicity, one-dimensional systems allow for a transparent discussion of the underlying physics. At the same time, experiments on S-TI-S junctions typically realize two-dimensional setups due to issues with confinement in one dimension. A two-dimensional S-N-S junction behaves qualitatively similar to its one-dimensional counterpart. It exhibits a transition from a minimal to a maximal thermal conductance at $\phi = \pi$ with increasing strength of the interface potential barrier, cf. Fig. 2(b). Since quasiparticles with oblique incidence experience an effectively higher potential barrier at the interface, the crossover occurs at smaller values of Z in the two-dimensional case. In a two-dimensional S-TI-S junction, only quasiparticles with normal incidence exhibit unit transmission while quasiparticles with oblique incidence can be backscattered. Nevertheless, the S-TI-S junction always exhibits a minimal thermal conductance at $\phi = \pi$, see Fig. 2(b). It originates from the fact that the heat current contribution for oblique incidence is geometrically suppressed compared to that for normal incidence. This leads to a dominant contribution of the topological Andreev bound state even in the two-dimensional case. This remarkable finding allows to distinguish between topological and trivial 4π modes in two-dimensional junctions. Further, the thermal conductance of a S-TI-S junction oscillates as a function of the barrier strength due to the formation of resonances at the interface. This is a unique feature of the scattering of Dirac quasiparticles. To summarize, we find that for short S-TI-S junctions there are clear signatures of helical Andreev bound states for both the one- and two-

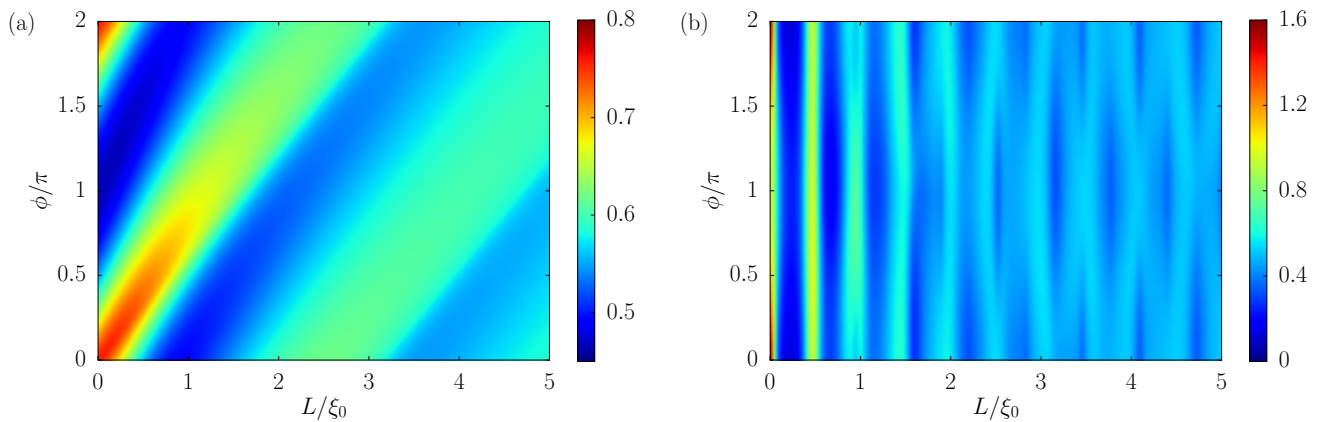


FIG. 3. (a) Thermal conductance of a long, one-dimensional S-TI-S Josephson junction in units of G_Q as a function of junction length L and phase difference ϕ for $k_B T = \Delta/2$. (b) Thermal conductance of a long, one-dimensional S-N-S junction in units of G_Q with $k_N = 0.1k_S$, $\hbar v_F k_S = 50\Delta$ and $k_B T = \Delta/2$.

dimensional case.

Long junction.— For a long, one-dimensional S-TI-S junction, the energy dependence of the electron and hole wave vector in the intermediate TI region, $k_{N,e/h} = k_N \pm \omega/(\hbar v_F)$, where k_N is the Fermi wave vector, gives rise to a modified transmission function,

$$\mathcal{T}_e(\omega, \phi) = \frac{\omega^2 - \Delta^2}{\omega^2 - \Delta^2 \cos^2\left(\frac{\phi}{2} - \frac{\omega L}{\hbar v_F}\right)}. \quad (7)$$

As a consequence, the maximal and minimal thermal conductance no longer occur at $\phi = 0$ and $\phi = \pi$, respectively but are shifted to finite values of ϕ , cf. Fig. 3(a). This is reminiscent of the ϕ -junction behaviour of the Josephson current in certain Josephson junctions with singlet and triplet pairing [28–37]. We remark that the ϕ -junction behavior of the thermal conductance here is due to the wave vector difference between electrons and holes and, thus, of a completely different origin than the ϕ -junction behavior of the Josephson current in the aforementioned junctions. Furthermore, the oscillations of the thermal conductance with ϕ are damped on the scale of the superconducting coherence length $\xi_0 = \Delta/(\hbar v_F)$.

For an S-N-S junction, the energy dependence of electron and hole wave vectors in the normal region of the junction also gives rise to a ϕ -junction behavior of the heat conductance just as for a S-TI-S junction. On top of this, the S-N-S junction exhibits Fabry-Pérot type oscillations that occur on a length scale k_N^{-1} due to finite scattering probabilities at the S-N interfaces. The interplay between these two effects gives rise to a complicated interference patterns, cf. Fig. 3(b). While the interference pattern makes it hard to extract information from the thermal conductance of a S-N-S junction, it allows for a clear distinction from helical Andreev bound states in a S-TI-S junction which do not exhibit Fabry-Pérot type oscillations as a consequence of Klein tunneling.

Possible experiment.— In order to experimentally verify our theoretical predictions, we suggest to use a SQUID consisting of two superconducting electrodes connected via identical S-TI-S Josephson junctions, cf. Fig. 1(a). The phase difference across the junctions can be controlled by a magnetic flux Φ through the SQUID. Normal metal electrodes connected to the superconductors via tunnel barriers serve as heater and thermometer, respectively. The heat flow in this setup can be accounted for in a simple thermal model, see Fig. 1(b), with the heat \dot{Q}_{heater} injected by the heater, the phase-dependent heat flow $\dot{Q}(\Phi) = 2\kappa(\phi)(T_L - T_R)$ through the two Josephson junctions as well as heat losses into the substrate due to electron-phonon coupling, $\dot{Q}_{\text{e-ph}}^r = 0.98e^{-\Delta/k_B T_r} \Sigma_r V_r (T_r^5 - T_{\text{bath}}^5)$, $r = L, R$ [38]. In the following, we assume an electron-phonon coupling strength of $\Sigma_r = 10^9 \text{ W m}^{-3} \text{ K}^{-5}$ and take the volume of each superconductor to be $V_r = 10^{-20} \text{ m}^3$ [18]. For a bath temperature of $T_{\text{bath}} = 100 \text{ mK}$, a temperature of the left superconductor $T_L = 500 \text{ mK}$ and a superconducting pair potential equal to twice the average electron temperature, we find that the temperature of the right superconductor varies between 360 mK and 380 mK for single-channel Josephson junctions. This variation is clearly within the reach of current experimental technology [18]. We remark that while the precise value of the temperature of the right superconductor depends on the exact values of parameters, the variation of about 20 mK is very robust with respect to parameter variations and occurs, e.g., also for a junction with many open transport channels.

Summary.— We demonstrated that the phase-dependent thermal conductance of a S-TI-S Josephson junction contains clear signatures of the existence of topological Andreev bound states. Importantly, the predicted effects are robust with respect to the

dimensionality and length of the junction. Furthermore, we have proposed an experimental setup that allows for the verification of our predictions using available SQUID devices. Our results pave the way to observe experimentally a clear difference between topologically trivial and nontrivial 4π modes.

We acknowledge financial support from the DFG via SFB 1170 "ToCoTronics", and the ENB Graduate School on Topological Insulators.

-
- [1] A. F. Andreev, *Sov. Phys. JETP* **19**, 1228 (1964).
 [2] A. F. Andreev, *Sov. Phys. JETP* **22**, 455 (1966).
 [3] C. W. J. Beenakker, *Phys. Rev. Lett.* **67**, 3836 (1991).
 [4] L. Fu and C. L. Kane, *Phys. Rev. Lett.* **100**, 096407 (2008).
 [5] L. Fu and C. L. Kane, *Phys. Rev. B* **79**, 161408 (2009).
 [6] L. Maier, J. B. Oostinga, D. Knott, C. Brüne, P. Virtanen, G. Tkachov, E. M. Hankiewicz, C. Gould, H. Buhmann, and L. W. Molenkamp, *Phys. Rev. Lett.* **109**, 186806 (2012).
 [7] J. B. Oostinga, L. Maier, P. Schüffelgen, D. Knott, C. Ames, C. Brüne, G. Tkachov, H. Buhmann, and L. W. Molenkamp, *Physical Review X* **3**, 021007 (2013).
 [8] I. Sochnikov, L. Maier, C. A. Watson, J. R. Kirtley, C. Gould, G. Tkachov, E. M. Hankiewicz, C. Brüne, H. Buhmann, L. W. Molenkamp, and K. A. Moler, *Phys. Rev. Lett.* **114**, 066801 (2015).
 [9] C. Kurter, A. D. K. Finck, Y. S. Hor, and D. J. Van Harlingen, *Nat. Commun.* **6**, 7130 (2015).
 [10] J. Wiedenmann, E. Bocquillon, R. S. Deacon, S. Hartinger, O. Herrmann, T. M. Klapwijk, L. Maier, C. Ames, C. Brüne, C. Gould, A. Oiwa, K. Ishibashi, S. Tarucha, H. Buhmann, and L. W. Molenkamp, *Nat. Commun.* **7**, 10303 (2016).
 [11] K. Maki and A. Griffin, *Phys. Rev. Lett.* **15**, 921 (1965).
 [12] K. Maki and A. Griffin, *Phys. Rev. Lett.* **16**, 258 (1966).
 [13] G. D. Guttman, B. Nathanson, E. Ben-Jacob, and D. J. Bergman, *Phys. Rev. B* **55**, 3849 (1997).
 [14] G. D. Guttman, E. Ben-Jacob, and D. J. Bergman, *Phys. Rev. B* **57**, 2717 (1998).
 [15] D. Golubev, T. Faivre, and J. P. Pekola, *Phys. Rev. B* **87**, 094522 (2013).
 [16] E. Zhao, T. Löfwander, and J. A. Sauls, *Phys. Rev. Lett.* **91**, 077003 (2003).
 [17] E. Zhao, T. Löfwander, and J. A. Sauls, *Phys. Rev. B* **69**, 134503 (2004).
 [18] F. Giazotto and M. J. Martínez-Pérez, *Nature* **492**, 401 (2012).
 [19] M. J. Martínez-Pérez and F. Giazotto, *Nat. Commun.* **5**, 3579 (2014).
 [20] A. Fornieri, C. Blanc, R. Bosisio, S. D'Ambrosio, and F. Giazotto, *Nature Nanotech. advance online publication* (2015), 10.1038/nnano.2015.281.
 [21] F. Giazotto and F. S. Bergeret, *Appl. Phys. Lett.* **102**, 132603 (2013).
 [22] F. S. Bergeret and F. Giazotto, *Phys. Rev. B* **88**, 014515 (2013).
 [23] P. Virtanen and F. Giazotto, *Phys. Rev. B* **90**, 014511 (2014).
 [24] P. Virtanen and F. Giazotto, *AIP Advances* **5**, 027140 (2015).
 [25] S. Spilla, F. Hassler, and J. Splettstoesser, *New J. Phys.* **16**, 045020 (2014).
 [26] G. Tkachov and E. M. Hankiewicz, *Phys. Rev. B* **88**, 075401 (2013).
 [27] G. Tkachov and E. M. Hankiewicz, *Phys. Status Solidi B* **250**, 215 (2013).
 [28] A. Buzdin, *Phys. Rev. Lett.* **101**, 107005 (2008).
 [29] A. Brunetti, A. Zazunov, A. Kundu, and R. Egger, *Phys. Rev. B* **88**, 144515 (2013).
 [30] T. Yokoyama, M. Eto, and Y. V. Nazarov, *Phys. Rev. B* **89**, 195407 (2014).
 [31] D. Feinberg and C. A. Balseiro, *Phys. Rev. B* **90**, 075432 (2014).
 [32] A. Buzdin and A. E. Koshelev, *Phys. Rev. B* **67**, 220504 (2003).
 [33] N. G. Pugach, E. Goldobin, R. Kleiner, and D. Koelle, *Phys. Rev. B* **81**, 104513 (2010).
 [34] E. Goldobin, D. Koelle, R. Kleiner, and R. G. Mints, *Phys. Rev. Lett.* **107**, 227001 (2011).
 [35] H. Sickinger, A. Lipman, M. Weides, R. G. Mints, H. Kohlstedt, D. Koelle, R. Kleiner, and E. Goldobin, *Phys. Rev. Lett.* **109**, 107002 (2012).
 [36] I. Kulagina and J. Linder, *Phys. Rev. B* **90**, 054504 (2014).
 [37] B. Sothmann and R. P. Tiwari, *Phys. Rev. B* **92**, 014504 (2015).
 [38] A. V. Timofeev, C. P. García, N. B. Kopnin, A. M. Savin, M. Meschke, F. Giazotto, and J. P. Pekola, *Phys. Rev. Lett.* **102**, 017003 (2009).